Outdoor fibre link between two telescopes and the lab of the CHARA array at 810 nm. Demonstration of the optical path servo control.

Julie Magri
XLIM
Ludovic Grossard (ludovic.grossard@unilim.fr)
XLIM
François Reynaud
XLIM
Marc Fabert
XLIM
Laurent Delage
XLIM
Rodolphe Krawczyk
Thales Alenia Space
Jean-Michel Le Duigou
Centre National d'Études Spatiales

Research Article

Keywords: Interferometry, Optical fibre, Long baseline, Servo control, High resolution imaging

Posted Date: September 9th, 2022

DOI: https://doi.org/10.21203/rs.3.rs-2014442/v1

Outdoor fibre link between two telescopes and the lab of the CHARA array at 810 nm. Demonstration of the optical path servo control.

Magri Julie[1], Grossard Ludovic[1*], Reynaud François[1], Fabert Marc[1], Delage Laurent[1], Krawczyk Rodolphe[2] and Le Duigou Jean-Michel[3]

[1]Univ. Limoges, CNRS, XLIM, UMR 7252, 123 Avenue Albert Thomas, Limoges, 87000, France.
[2]Thales Alenia Space, Observation Exploration & Navigation, 5 Allée des Gabians BP 99, Cannes La Bocca Cedex, 06156, France.
[3]CNES, Centre Spatial de Toulouse, Service DSO/SI/OP, 18 avenue Edouard Belin, Toulouse Cedex 09, 31401, France.

*Corresponding author(s). E-mail(s): ludovic.grossard@unilim.fr;
Contributing authors: julie.magri@xlim.fr;
francois.reynaud@unilim.fr;

Abstract

In the framework of the ALOHA (Astronomical Light Optical Hybrid Analysis) project, dedicated to high resolution imaging in the L-band using optical fibre and nonlinear optics, we have implemented a servo controlled hectometric outdoor fibre link between two telescopes and the recombination beam facility of the CHARA telescope array. A two-stage servo system using optical fibre modulator, fibre delay line, and a metrology laser at 1064 nm allows to stabilise the optical path difference within 3 nm RMS over a 3000 s record. Using an internal source at 810 nm, the signal-to-noise ratio of the fringe modulation peak is enhanced by a factor better than two when the servo control is switched on. This study can be also considered as a seminal work towards very long base fibre linked telescope arrays and allows to scale the perturbative environment of an outdoor fibre link.

Keywords: Interferometry, Optical fibre, Long baseline, Servo control, High resolution imaging

1 Introduction

The possibility to design and implement a very large telescope array is a crucial quest for high-resolution imaging. The usual way to propagate the beams from the distant telescopes to the mixing station uses a mirror train. This method is robust, but induces very high losses due to the large number of reflections (typically in the range of 20) and involves a very demanding global mirror alignment process. In addition, the longer the baseline, the larger the beam diameter to minimise the diffraction impacts all over the interferometric arms. To overcome these difficulties, the use of single mode fibres has been proposed very early in the 80's (Connes et al, 1985). After injection of the light at each telescope focus, the spatial filtering allows to get highly calibrated fringes, as demonstrated in various recombining instruments like FLUOR (Coudé du Foresto et al, 2003), MIRC (Monnier et al, 2006) or SPICA (Mourard et al, 2018). This experimental configuration reduces the number of freedom degree to be controlled, limits the diffraction effects at the propagation in the delay lines and significantly enhances the overall throughput of the instrument thanks to the tremendous performances of the fibre optic transmission. However, to take advantage of this new instrumental scheme, it is necessary to manage the dispersion, polarisation and optical path difference stability behaviours. First two points have been extensively studied in laboratory, and robust experimental configurations have been proposed to manage the compensation of differential effects between the interferometric arms (Lagorceix and Reynaud, 1995), (Vergnole et al, 2005). The only successful on-site fibre link on a long baseline was demonstrated in 2005 between the two Keck telescopes (Hawaii, USA), but the fibres were laid indoor and without any Optical Path Difference (OPD) stabilisation (Perrin and al., 2006). To address the issue of on-site OPD stabilisation in an outdoor configuration, preliminary results (Lehmann et al, 2019) were obtained with a Mach-Zehnder fibre-optic interferometer fed by an internal source, and installed at the Center for High Angular Resolution Astronomy (CHARA) Array site located at the top of Mount Wilson (Brummelaar et al, 2005), but without taking into account the fibre path in the telescope and with a limited correction range.

In this paper, we present the complete implementation of a fibre link between the two telescopes S1 (South 1) and S2 (South 2) and the CHARA beam combination laboratory. The 240 m long fibres are laid outdoor on the ground with simple foam insulation and a protective layer of PVC pipe. The fibres reach the focusing stage of the telescope passing though the cable wrap, taking care to mitigate the stresses applied to the optical fibre. A metrology interferometer using a two-stage servo loop is used to stabilise the piston i.e. the OPD fluctuation. Low frequency correction is achieved by a stepper motor

driving a fibre delay line, while a fast stage using a piezoelectric drives a fibre optical path modulator. When operated in real conditions, including telescope and dome motions, we demonstrate the stabilisation of the OPD to within 10 nm over more than one hour.

2 General experimental configuration

The reported experiment is developed at the Mount Wilson Observatory (USA, CA), in the framework of a collaboration between the XLIM and CHARA teams. The goal of this demonstration of a fibre link with long outdoor fibres is twofold.

First, it's a major step of the global ALOHA project (Lehmann et al, 2018) which aims to promote the joint use of nonlinear optics and high resolution imaging for astronomy. The infrared or mid-infrared light is shifted to a shorter wavelength thanks to a sum frequency nonlinear process (Boyd, 1977) so that the converted light can efficiently propagate through optical fibres towards the CHARA's delay lines to be mixed. Our experimental setup is shown in figure 1. The astronomical light wavelength initially around 3.5 µm is shifted near 810 nm after mixing with a 1064 nm laser pump. This way, the fibre link is designed around 810 nm.

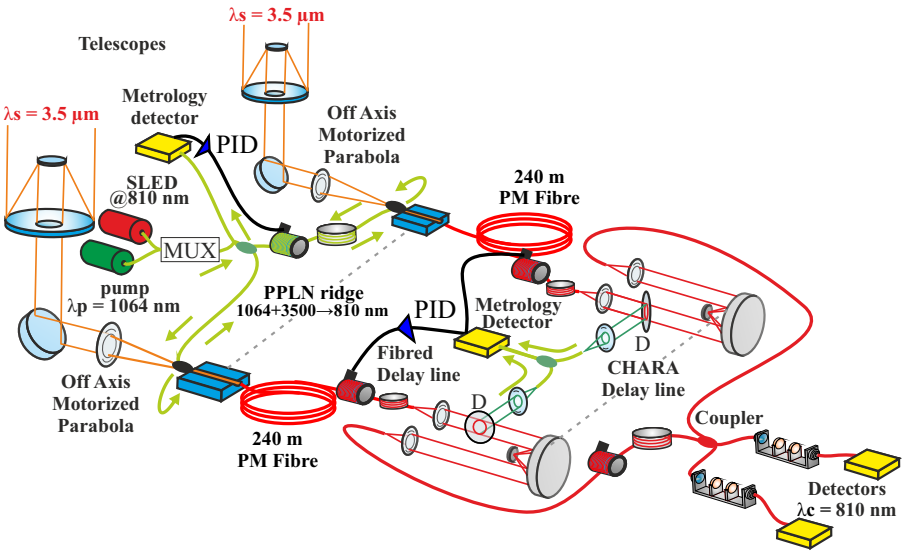

Fig. 1 ALOHA at CHARA: the astronomical light collected by the S1 and S2 telescopes at 3.5 µm is converted to 810 nm at each telescope thanks to a nonlinear PPLN crystal and a pump laser beam at 1064 nm routed through two 50-metre optical fibres. The converted fields are then propagated in 240 metre long optical fibres whose lengths are servo controlled. The converted signals coming out of the fibres pass through CHARA's free space delay lines before the mixing stage to get fringes as a function of time. The interferometric mixing is finally detected by photon counting detectors after passing through a narrow-band filter.

Second, this 810 nm fibre link can be seen as a precursor of the extended CHARA array Michelson project (Gies et al, 2019) and will allow to scale the environmental issues due to thermal and vibration disturbances.

In both cases, a servo control of the OPD is mandatory. In the following, we will describe the ALOHA configuration. The corresponding metrological scheme is illustrated on figure 2 and consists of two main blocks with a Michelson and a Mach-Zehnder structures described in the following paragraphs.

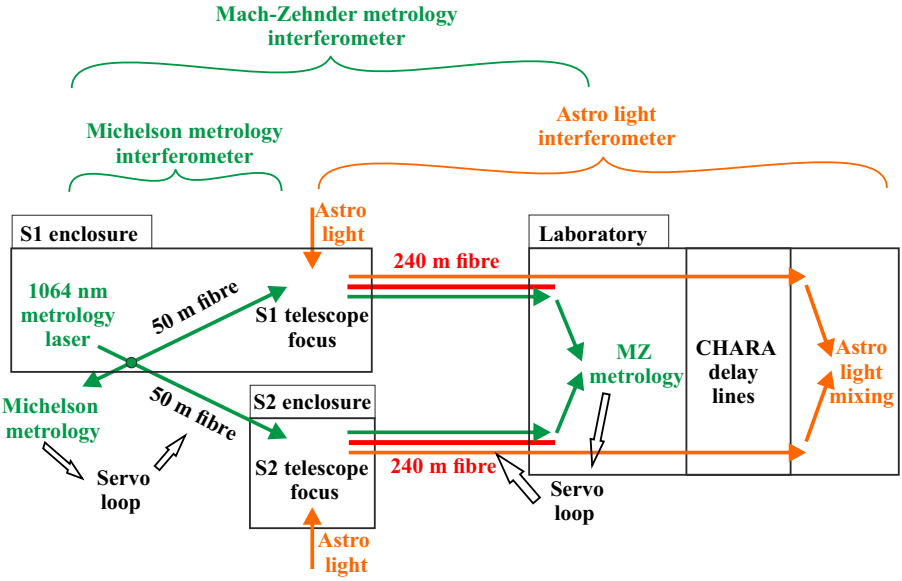

Fig. 2 Synoptic scheme of the servo control system. The first servo control has a Michelson interferometer structure used for metrology. It allows to stabilise the 50 metre optical fibres which share the pump at 1064 nm towards the focus of each of the two telescopes. The second servo control uses a Mach-Zehnder interferometer. It is used to stabilise the 240 metres of optical fibres collecting the astronomical light for the two configurations, with or without conversion.

The optical paths to be servo controlled for astronomical light correspond to the sections from the telescopes focal points to the inputs of the delay lines. The foci of the telescopes are separated by distances of up to several hundred metres. This way, it is necessary to provide a phased metrology signal for each telescope. In the framework of the ALOHA project, the nonlinear processes requires sharing the same pump laser field to preserve the coherence properties of the converted signals. The light from this pump laser can be therefore used as a metrology signal to control the OPD between the two 240 m fibre.

2.1 The Michelson interferometer: generation of cophased reference beams

The first part of the metrology setup is a Michelson interferometer, as shown in figure 3. Its input is located in S1, where the field emitted by a 1064 nm distributed-feedback laser is injected into a 50/50 fibre coupler to share the pump light equally between two 50 m single-mode Polarisation Maintaining (PM) fibres at 1064 nm that deliver the pump waves to the S1 and S2 telescope foci.

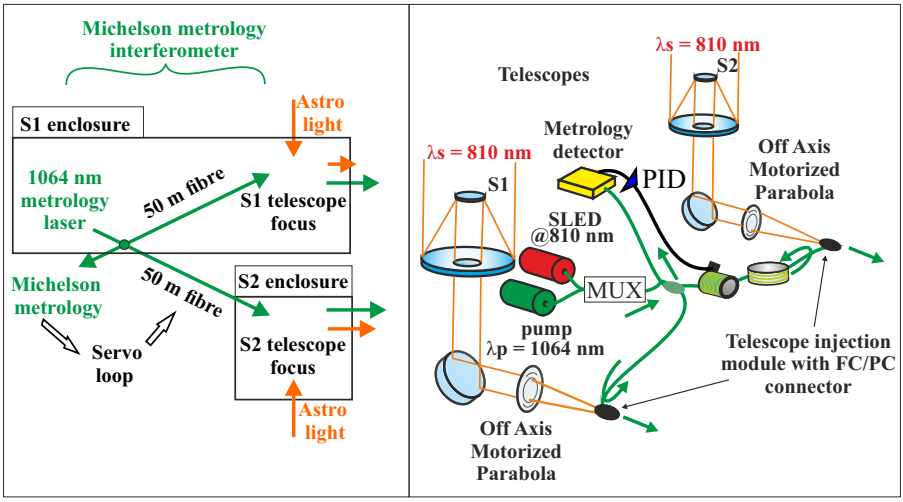

Fig. 3 Michelson stage of the servo control system: light of a metrology/pump laser at 1064 nm is equally shared between the two 50 m fibres. Most of the flux is transmitted to the Mach-Zehnder stage, but a few percent are back reflected to generate the error signal by detecting interferometric mixing. A PID filter and an amplifier are used to drive a fibre optic modulator to correct the optical path fluctuations. A monitoring of the correction and a fibre delay line are used to desaturate the optical path modulator stage.

The first fibre remains in the S1 basement, passes through the S1 cable wrap and reaches the S1 Adaptive Optics (AO) table where starlight is available. The second 50 m fibre section goes from S1 to S2 through an outside path, then passes through the S2 cable wrap stage and reaches the S2 telescope AO table. All connectors are FC/APC to avoid any backward reflection, except at both ends of the fibres in S1 and S2, where a FC/PC connector is inserted to send back a small part (5 percent Fresnel reflection) of the flux to the coupler. The second coupler input is used as the Michelson interferometer output, and the interferometric mixing is detected by an InGaAs photodiode. The error signal is generated by removing the DC part of the interferometric signal. A PID filter processes the error signal to provide the correction signal that drives a fibre optic modulator after passing through a high voltage (HV) amplifier. In our experimental configuration, this fast correction has a span in the range of 50 µm. The HV amplifier/ optical path modulator is then desaturated by a

slow fibre delay line driven by a servo system if the correction signal exceeds operating boundaries, as show in figure 4. This two-level correction makes it possible to manage sub-wavelength accuracy over the 20 mm stroke of the fibre delay line.

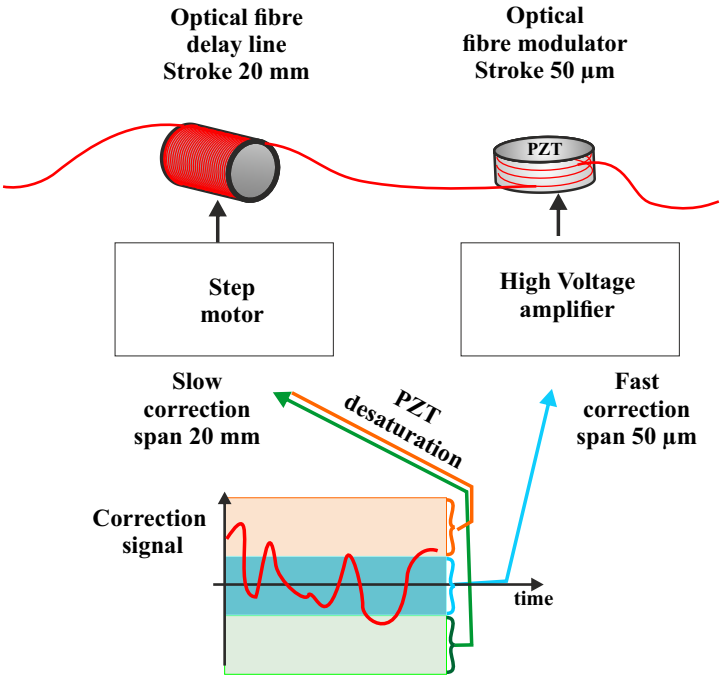

Fig. 4 The correction of the optical path fluctuation is achieved by a two stage actuator: an optical fibre delay line with a 20 mm stroke (left) and an optical fibre modulator with a 50 µm correction range (right). The latter manages the fast correction over a limited correction signal range (blue). If the correction signal goes out of this blue correction range (orange and green) the optical fibre delay line is activated to desaturate the fibre modulator.

When the servo is turned on, the pump signals delivered at the telescope foci are phase locked and available to perform the S1, S2 to Laboratory fibre link servo control system.

2.2 The Mach-Zehnder interferometer: stabilisation of the 240 m long fibre optical paths

The Michelson interferometer described in the previous section acts as a beam splitter for the Mach-Zehnder interferometer which aims to servo the two 240 m long fibres. The two fields transmitted through the Michelson reflectors (FC/PC connectors) are phase-locked, and are used as metrology inputs for the two fibres connecting the S1 and S2 telescopes to the laboratory.

The injection stage is shown in figure 5. A dichroic plate allows to simultaneously inject the star light and the metrology laser light in the fibre. The

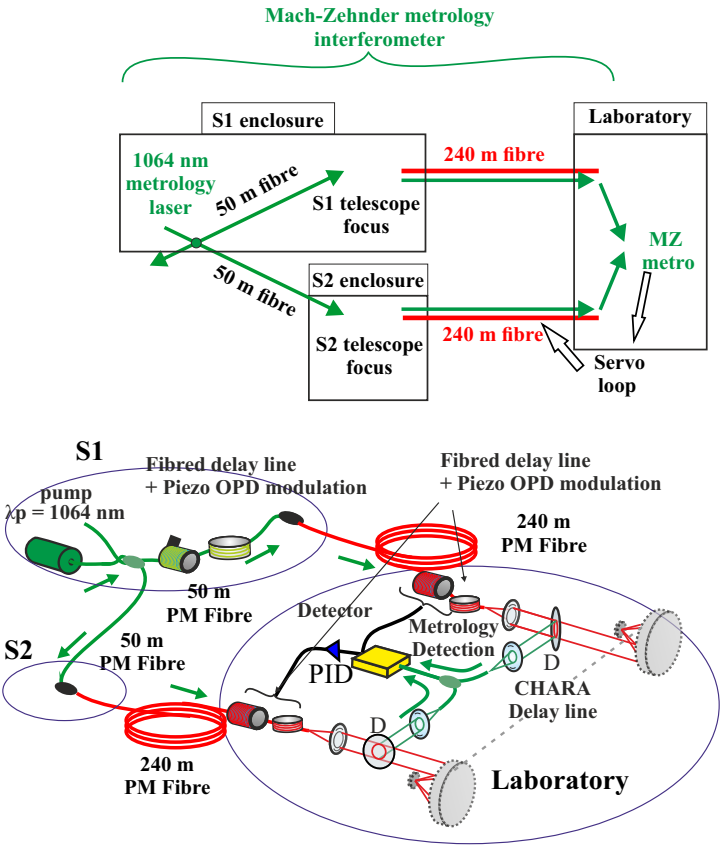

Fig. 5 Schematic and drawing of the Mach-Zehnder metrology interferometer: the two arms of the interferometer are fed by the outputs of the upstream Michelson interferometer. The metrology beams then pass through the two 240 m fibres, and reach the inputs of the CHARA delay lines. They are then captured by dichroic plates D and mixed by a fibre coupler. The resulting interferometric signal is processed in the same way as for the Michelson metrology interferometer, using a two-level correction (fibre modulator plus delay lines) on each arm of the interferometer, in a push-pull configuration.

astronomical light around 800 nm and the metrology signal at 1064 nm travel simultaneously in the two waveguides. In each telescope, the 240 m-long fibre route passes through the cable wrap in the telescope enclosure, where it is held by a tubular sling supported by stainless steel cable to relieve stresses applied to the fibre. All along the fibre link, the fibre is packed in a 3 mm furcation tubing embedded in a 10 mm diameter flexible stainless steel conduit. For all the outdoor sections, the fibre is laid on the ground and wrapped in an insulating pipe protected by a PCV tube. The fibre cables pass through the laboratory hall to reach the entrance of the CHARA delay lines, close to the periscopes used in the classical mirror train configuration. Two collimation assemblies are installed on the CHARA delay line rails. At the output of each fibre, the 810 nm light is collimated to the CHARA delay lines, while

the 1064 nm metrology light is collected through a dichroic plate, and injected into a fibre mixing coupler. The resulting metrology interferometric signal is used to generate an error signal after removing the DC component. A PID filter and a power amplifier drive optical path modulators implemented on each 240 m fibre section to correct OPD fluctuations in a push-pull configuration. In parallel, a fibre optic delay line allows to desaturate fibre optic modulator with the same scheme as for the Michelson stage.

2.3 Internal source and fringes

In order to test the efficiency of the servo control system, the interferometer is tested internally by injecting a broadband source with a spectrum around 810 nm, as shown in figure 6. A 1064 nm / 810 nm fibre multiplexer mixes the 810 nm radiation and the metrology signal so that the 810 nm radiation propagates along the same path as the metrology light to the dichroic plates at the CHARA delay lines inputs. After passing through the dichroic plates, the 810 nm optical fields are sent into the CHARA delay lines and then mixed by a fibre coupler.

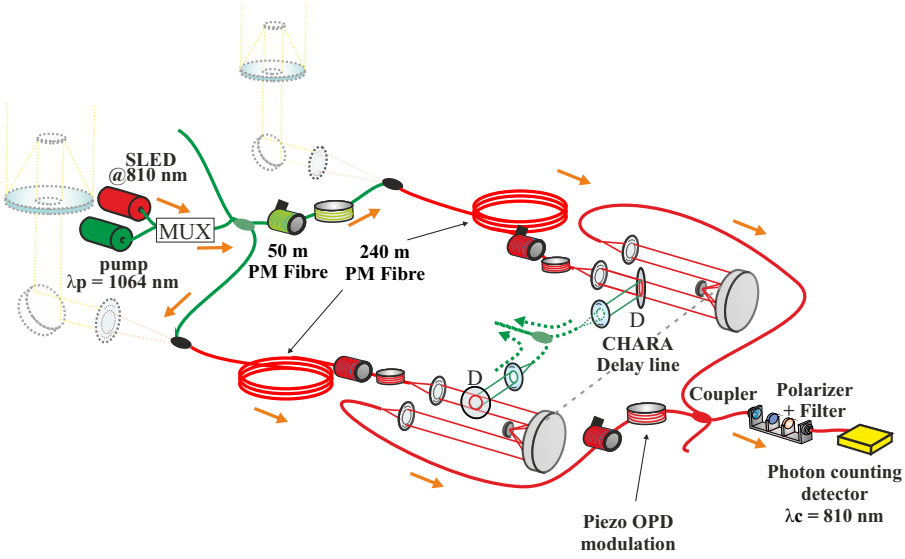

Fig. 6 Internal fringe configuration: the light emitted by a Superluminescent Diode (SLED) used as an internal source passes through the 50 m pump fibres to reach the S1 and S2 telescopes where it is injected into the 240 m fibres and routed into the CHARA laboratory building. The emerging optical beams are sent through the CHARA's free-space delay lines before being mixed, filtered and detected by a photon counting detector. This set up allows us to search for the zero optical path difference of the fibre link by scanning the OPD with the CHARA delay lines.

At the output of the 810 nm interferometer, the fringes are displayed as function of time using a fibre optic modulator. A narrow band filter allows to

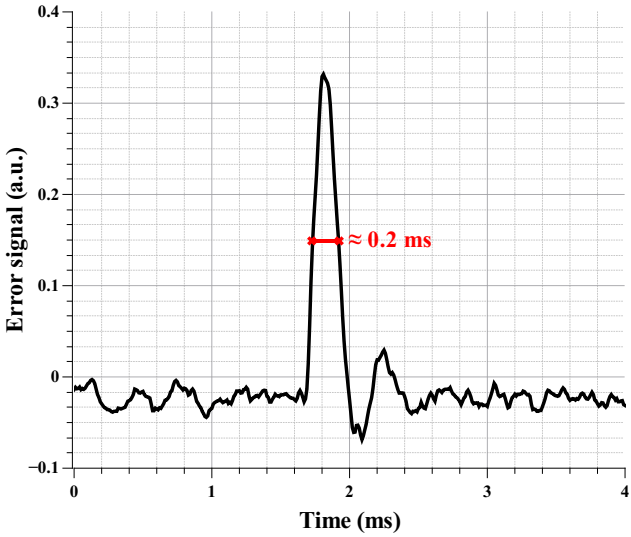

Fig. 7 Response time of the Michelson metrology interferometer servo control system. An external electronic perturbation (Heaviside shape) is used to characterise the time taken to reach the operating point. The response time is about 0.2 ms FWHM.

adjust the coherence length of the detected interferogram to the optical path modulation of each temporal scan. The recorded signal is Fourier Transformed to get the fringe pattern spectrum. An averaging process is then applied on the square modulus of this spectrum to fit the same signal processing conditions as on the sky. By adjusting the free space CHARA delay lines, it is possible to find the zero optical group delay with this internal fringes configuration. As the two sets of fibres have been equalized in length with an accuracy in the order of mm, the real interferometer is ready to be used on the sky with fringes position close to zero OPD.

3 Experimental results

3.1 The Michelson interferometer: generation of cophased reference beams

In a first step, we determined the response time of the Michelson interferometer stabilisation system. A Heaviside electronic perturbation is injected into the servo loop in order to measure the response time required to stabilise the interferometer at the operating point. The experimental results show a typical 0.2 ms response time FWHM, as shown in figure 7, which is fully compatible with the OPD temporal fluctuations to be corrected.

In a second step, the short-term stability is analysed over a 100 ms frame (figure 8). The RMS fluctuation of the OPD is around 3 nm when the servo control is ON, i.e. in the range of $\lambda/300$ at the metrology wavelength.

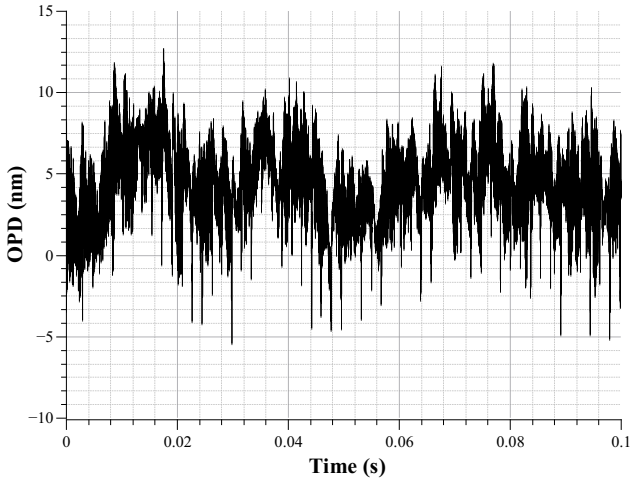

Fig. 8 Michelson stage short-term stability over a 100 ms frame: the calibration of the fringe amplitude allows to derive the residual OPD fluctuation with a 3 nm RMS value when the servo is ON.

In the previous experiment (Lehmann et al, 2018) the correction was only applied by the piezo optical fibre modulator, leading to servo stalling due to a limited stroke of the correction actuator. In our new servo system, the adjustable delay line allows to desaturate the piezo so that the servo control system benefits from the high accuracy piezo correction all over the delay line stroke. The delay line voltage applied to the piezo is monitored to remain within a ±24 V voltage range (corresponding to a correction signal between -2 V and +2 V before amplification with a gain equal to 12). Fig. 9 plots simultaneously the optical path correction applied by the optical fibre modulator (black) and the delay line position (red). As the delay line compensates for the main drift during the record, it is a good way to characterise the environmental disturbance to be corrected. Note that, experimentally, we have observed a fluctuation of less than one millimetre for the 50 m long fibre set used in the Michelson interferometer. The small peaks on the black curve correspond to dome motions that are well corrected. Conversely, the significant transient behaviour in the middle of the graph corresponds to a rapid slewing of the telescope and its dome when moving from one astronomical target to another. Of course, during these non observation periods, the servo is not effective. These results demonstrate the efficient operation of optical path servo control of the two 50 m long fibres included in the Michelson configuration with an accuracy of a few nanometres. This way, it is possible to provide phase-locked optical fields to stabilise the 240 m fibre sections.

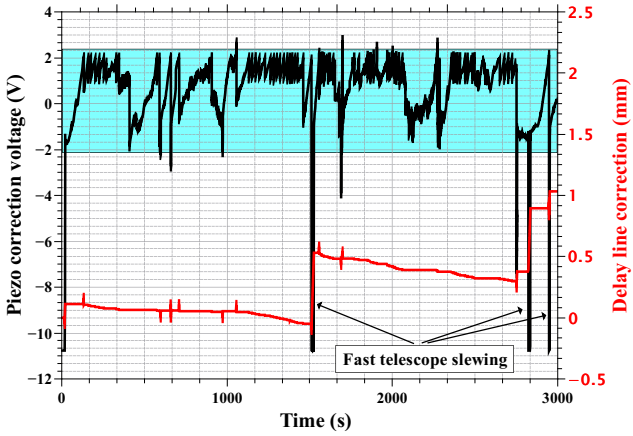

Fig. 9 Michelson interferometer long-term stability. Black: optical path correction applied on the optical fibre modulator, red: delay line position.

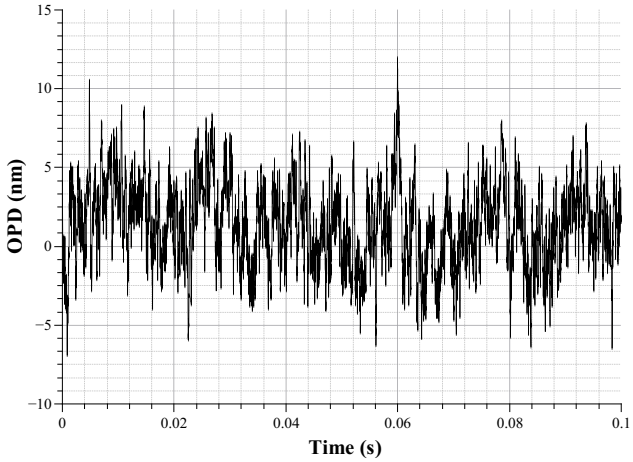

Fig. 10 Mach-Zehnder short-term stability over a 100 ms frame: the calibration of the fringe amplitude allows to derive the residual optical path fluctuation with a 3 nm RMS value when the servo is ON.

3.2 The Mach-Zehnder interferometer: optical path servo of the 240 m long fibres

Firstly, the response time tests on the Mach-Zehnder stage show identical results to those of the Michelson, with a typical transient behaviour of 0.2 ms. Secondly, a short-term optical path stability of 3 nm RMS is measured when the servo is switched on, as shown in figure 10. This demonstrates that the servo control system is fully appropriate for the stabilisation of the interferometer.

Fig. 11 and 12 describe the long-term evolution of the correction signal applied to the piezoelectric modulator, and of the optical fibre delay line position. Fig. 11 focuses on the first 200 seconds of servo monitoring. During the first 20 seconds the servo is off, the correction signal (black curve) is saturated and the delay line (red curve) is set to the reference position. When the servo is switched on (point A), the correction reaches the operating range (blue area) and the delay line moves to the 0.12 mm position. Between points A and B, the correction signal changes from -2 V to 2 V to compensate for OPD fluctuations. The delay line remains at the same position. At point B, the delay line adjustment is applied to desaturate the correction. This process is applied again at points C and D.

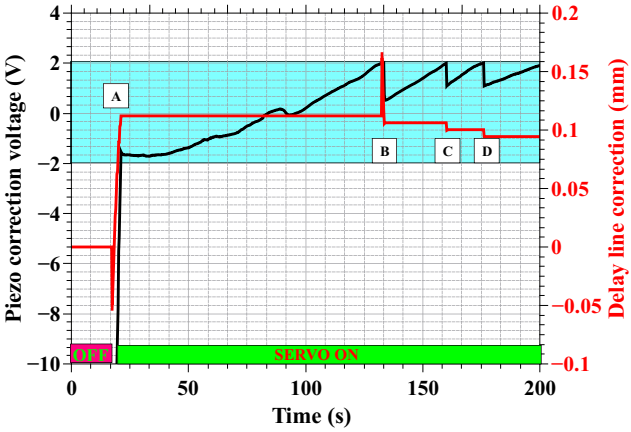

Fig. 11 Correction voltage and delay line position at the beginning of the Mach-Zehnder servo operation during the first 200 s of operation. At point A: servo switched ON, at points B, C and D: the delay line desaturate the correction

Fig. 12 shows the evolution of the correction voltage and delay line position over 3000 s during the night of 03/19/2022. The servo control system operated successfully over two 1400 second slots. The only transient behaviour at 1400 s and 2800 s correspond to the rapid slewing of the telescope when moving from one target to another. During these two steps, the servo stalls and induces a small shift (about 0.5 mm) in the position of the delay line(red curve). This minor shift can be easily compensated by the CHARA delay lines using internal fringes, as explained in the next paragraph.

3.3 Internal fringes: Calibration of the optical path difference

In order to calibrate the optical path difference between the two 240 m fibre arms, a broadband source (SLED) emitting around 810 nm is injected through the Michelson and Mach-Zehnder interferometer cascade using a multiplexer

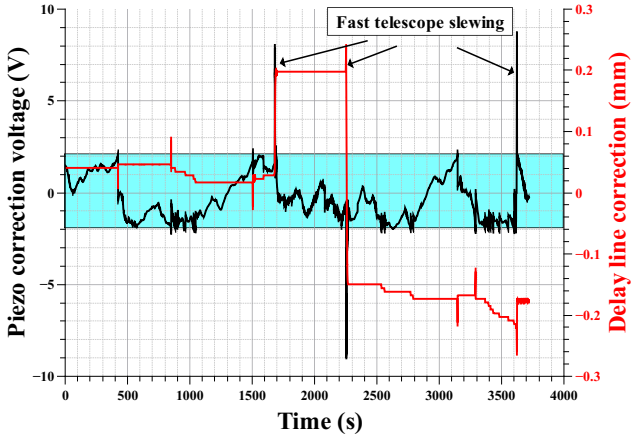

Fig. 12 Correction voltage and delay line position of the Mach-Zehnder servo during a 3000 s operation: The global operation is similar to figure 11. The servo was only stalled when the telescope was slewing fast from one target to another (at times 1400 s and 2800 s).

as described in the related paragraph (2.3). In a first step, we searched for the internal fringes around the supposed zero OPD by scanning over ±5 mm using the CHARA delay lines. In a second step, we measured the electrical pulses generated by the photon counting detector as a function of time around the zero OPD thanks to the piezo electric modulator (situated just before the output coupler). The raw data were achieved over a 500 frame integration with 0.2 s duration per frame, and the fringe modulation frequency was set to 175 Hz (35 fringes per temporal frame).

Fig. 13 shows the averaged Power Spectral Density (PSD) of the raw dataset in two configurations: when the servo controls of the Michelson and Mach-Zehnder interferometers are switched off (black curve), then when they were switched on (red curve). Both curves show the presence of a modulation peak on spectral channel 35 as expected. Moreover, the modulation peak is sharper and higher when the servos are ON, clearly demonstrating the efficiency of the two fibre-length control systems.

To quantify the impact of fibre length servo on the characteristics of the fringe peak, we calculated the signal-to-noise ratio (SNR) defined by the ratio between the amplitude of the fringe peak in the PSD and the RMS value of the background fluctuations far from the fringe peak. Table 1 shows the SNR value calculated:

- by measuring the fringe peak amplitude at spectral channel 35,
- by integrating the whole fringe peak over several spectral channels.

In both cases, the SNR is improved by a factor greater than 2 when the servo controls are activated. This also demonstrates the improvement brought about by the use of servo systems.

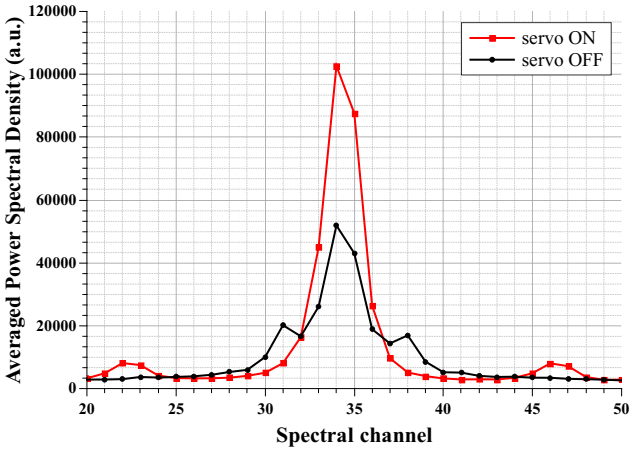

Fig. 13 Fringe spectrum, integrated over 500 frames of 0.2 s, when the servo is off (black curve) and on (red curve). The efficiency of the servo control system is demonstrated by a sharper and enhanced fringe peak.

Table 1 Signal-to-noise ratio of the fringe peak with and without servo-control after temporal integration over 500 frames of 0.2 s

	Servo ON	Servo OFF	SNR Ratio
SNR measured at channel 35	1331	579	2,3
SNR by integrating the fringe peak	1890 [a]	929 [b]	2,03

[a] obtained by peak integration over 3 spectral channels.
[b] obtained by peak integration over 9 spectral channels.

4 Conclusion and perspectives

In this paper, we have experimentally demonstrated the possibility of implementing an outdoor fibre link in the framework of the CHARA telescope array. We have proposed a two-stage servo control system whose architecture is compliant with the ALOHA experiment, which aims to promote the joint use of high resolution imaging telescope array, fibre-based light transport and spectrum conversion through nonlinear optics. This experiment demonstrated a very good optical path stabilisation in a range of a few nm and a response time of about 0.2 ms, compatible with the spectrum of disturbances to be corrected. Thanks to the reliability of the servo systems, the fringe position remains within a millimetre range around the operating position. This reliability is a key point to find the fringes without wasting time by performing long span scans. We are now ready to test on the sky our ALOHA instrument in two steps. First, without frequency conversion, to find the zero optical path at 810 nm. Second, with frequency conversion using the nonlinear stage, to complete the proof of principle of the ALOHA project on the CHARA array.

This kind of servo control system will be one of the key technologies necessary for the deployment of the new very large telescope array of the future CHARA kilometric infrared interferometer (Gies et al, 2019). In this context, the interferometric architecture proposed by F. Reynaud (Reynaud et al, 1992) in the 90's could be used. In this architecture, the optical length of each arm of the fibre link array is compared with a reference fibre. All the electronics for the two-stage correction system could be identical to the one reported in this paper.

Acknowledgments. This work has been supported by the Centre National d'Études Spatiales (CNES), Thales Alenia Space and the Institut National des Sciences de l'Univers (INSU). We would also like to thank the entire CHARA team for the help and support they gave us during the mission at CHARA.

Declarations

Authors' contributions

- Funding acquisition: Grossard Ludovic, Reynaud François, Krawczyk Rodolphe, Le Duigou Jean-Michel
- Experimental implementation and data collection: Magri Julie, Grossard Ludovic, Reynaud François, Fabert Marc
- Writing - original draft preparation: Reynaud François
- Writing - review and editing: Magri Julie, Grossard Ludovic, Reynaud François, Fabert Marc, Delage Laurent
- Supervision: Krawczyk Rodolphe, Le Duigou Jean-Michel

All authors read and approved the final manuscript.

Competing interests

Not applicable.

Funding

This work has been financially supported by the Centre National d'Études Spatiales (CNES), Thales Alenia Space and the Institut National des Sciences de l'Univers (INSU).

References

Boyd RW (1977) Infrared upconversion for astronomy. Optical Engineering 16(6):166,563–166,563. URL http://opticalengineering.spiedigitallibrary.org/article.aspx?articleid=1221458

Brummelaar TAt, McAlister HA, Ridgway ST, et al (2005) First Results from the CHARA Array. II. A Description of the Instrument. The Astrophysical Journal 628(1):453. https://doi.org/10.1086/430729, URL http://iopscience.iop.org/0004-637X/628/1/453

Connes P, Froehly C, Facq P (1985) A fiber-linked version of project TRIO. In: Longdon N, Melita O (eds) Kilometric Optical Arrays in Space

Coudé du Foresto V, Borde PJ, Merand A, et al (2003) FLUOR fibered beam combiner at the CHARA array. Proceedings of SPIE 4838:280–285. https://doi.org/10.1117/12.459942, URL http://dx.doi.org/10.1117/12.459942

Gies D, Brummelaar Tt, Schaefer G, et al (2019) The chara michelson array: A kilometer-sized optical/infrared interferometer. Bulletin of the AAS 51(7). URL https://baas.aas.org/pub/2020n7i226, https://baas.aas.org/pub/2020n7i226

Lagorceix H, Reynaud F (1995) Birefringent effect measurement and compensation in a highly birefringent fiber optical path modulator. Optics Communications 118(3-4):235–240. https://doi.org/10.1016/0030-4018(95)00237-3, URL https://linkinghub.elsevier.com/retrieve/pii/0030401895002373

Lehmann L, Darré P, Szemendera L, et al (2018) ALOHA—astronomical light optical hybrid analysis. Experimental Astronomy 46(3):447–456. https://doi.org/10.1007/s10686-018-9585-2, URL http://link.springer.com/article/10.1007/s10686-018-9585-2

Lehmann L, Delage L, Grossard L, et al (2019) Environmental characterisation and stabilisation of a 2×200-meter outdoor fibre interferometer at the CHARA Array. Experimental Astronomy https://doi.org/10.1007/s10686-019-09627-x, URL http://link.springer.com/10.1007/s10686-019-09627-x

Monnier JD, Pedretti E, Thureau N, et al (2006) Michigan Infrared Combiner (MIRC): commissioning results at the CHARA Array. In: Monnier JD, Schöller M, Danchi WC (eds) Advances in Stellar Interferometry, International Society for Optics and Photonics, vol 6268. SPIE, p 62681P, https://doi.org/10.1117/12.671982, URL https://doi.org/10.1117/12.671982

Mourard D, Berio P, Clausse JM, et al (2018) SPICA, a new 6T visible beam combiner for CHARA: science, design and interfaces. In: Mérand A, Creech-Eakman MJ, Tuthill PG (eds) Optical and Infrared Interferometry and Imaging VI. SPIE, Austin, United States, p 55, https://doi.org/10.1117/12.2311869, URL https://www.spiedigitallibrary.org/conference-proceedings-of-spie/10701/2311869/SPICA-a-new-6T-visible-beam-combiner-for-CHARA/10.1117/12.2311869.full

Perrin G, al. (2006) Interferometric Coupling of the Keck Telescopes with Single-Mode Fibers. Science 311(5758):194–194. https://doi.org/10.1126/science.1120249, URL http://adsabs.harvard.edu/abs/2006Sci...311..194P

Reynaud F, Alleman JJ, Connes P (1992) Interferometric control of fiber lengths for a coherent telescope array. Applied Optics 31(19):3736–3743. https://doi.org/10.1364/AO.31.003736, URL https://www.osapublishing.org/abstract.cfm?uri=ao-31-19-3736

Vergnole S, Kotani T, Perrin G, et al (2005) Calibration of silica fibers for the Optical Hawaiian Array for Nanoradian Astronomy ('OHANA): Temperature dependence of differential chromatic dispersion. Optics Communications 251(1–3):115–123. https://doi.org/10.1016/j.optcom.2005.02.077, URL http://www.sciencedirect.com/science/article/pii/S0030401805002129